High Bandwidth Tilt Measurement Using Low-Cost Sensors

John Leavitt, *Member, IEEE*, Athanasios Sideris, *Member, IEEE*, and James E. Bobrow, *Member, IEEE*

***Abstract*—In this paper, a state estimation technique is developed for sensing inclination angles using low-cost sensors. A low-bandwidth tilt sensor is used along with an inaccurate rate gyro and a low-cost accelerometer to obtain the measurement. The rate gyro has an inherent bias along with sensor noise. The tilt sensor uses an internal pendulum and therefore has its own slow dynamics. These sensor dynamics were identified experimentally and combined to achieve high-bandwidth measurements using an optimal linear state estimator. Potential uses of the measurement technique range from robotics, to rehabilitation, to vehicle control.**

***Index Terms*—Angle gyro, inclinometer, orientation estimation, pose estimation.**

I. Introduction

MANY modern mechanical control systems use orientation feedback relative to an inertial reference frame. For systems connected to the ground by a hinge or revolute joint, measuring orientation is not difficult since an encoder can be attached between ground and the rotating link to directly give orientation. However, for any untethered system, or one that can move about freely in space, determining its orientation is not trivial. In our case, we are designing a hopping robot with a single actuator, capable of balancing despite inherent open-loop instability [5]. This robot requires accurate orientation and rate feedback at a relatively high bandwidth to achieve stable balance control. In this paper, we develop a state-space estimation approach that produces a high-bandwidth orientation or tilt signal using inexpensive components. We focus our attention on planar motions, since sensing in three dimensions first requires sensing in the plane [6].

One option for planar orientation measurement is the use of a tilt sensor, such as a pendulum-type inclinometer, but these sensors have their own dynamics with limited bandwidth and therefore cannot provide the correct tilt information at high frequencies. Another approach is to use a gyroscope to infer the tilt angle of the robot. In theory, integrating the angular velocity output of a gyroscope (hereafter referred to as a gyro or rate gyro) should provide an accurate tilt angle, even when the system is moving quickly. In practice, low-cost gyros have an unknown bias (offset) and/or scaling in their output, as well as signal noise. Integrating the gyro output results in an angle estimate plus a drift term. This means that it is not practical to sense inclination angle from a gyro alone.

Manuscript received January 14, 2004; revised March 25, 2005. Recommended by Technical Editor H. Hashimoto.

The authors are with the Department of Mechanical and Aerospace Engineering, University of California, Irvine, CA 92697 USA (e-mail: leavittj@uci.edu; asideris@uci.edu; jebobrow@uci.edu).

Digital Object Identifier 10.1109/TMECH.2006.875571

Another approach is to use a two-axis accelerometer to measure the direction of the gravity in a rotating reference frame [7]. Because accelerometers have a relatively high bandwidth and low cost, they are often used in this manner as tilt sensors. In practice, however, we have found them to be sensitive to vibrations, and relatively difficult to use since they require a nonlinear arctangent evaluation in the control loop. Ojeda and Borenstein [4] used accelerometers as tilt sensors to reset their gyros when their robot is not moving. They also found that vibrations during motion were problematic. More recently, Rehbinder and Hu [3] developed a switching state estimator for sensing attitude in three dimensions. Their approach combines gyro and acceleration measurements, and switches the estimator rely mostly on the gyro signal when the magnitude of the acceleration vector is high. They noted the problem of a bias signal from the gyros, but were not able to eliminate it. Our approach solves this problem with the use a tilt sensor that provides enough extra information for the state estimator to determine the bias online.

The state estimator developed in this work combines data from a gyro, a pendulum inclinometer, and a two-axis accelerometer to estimate the tilt angle. We used a U.S. Digital T2-7200-T optical inclinometer (cost $\approx$ \$100, U.S. Digital Corporation), along with a Murata ENC-03JA piezo gyroscope (cost $\approx$ \$50, Murata Manufacturing Companey, Ltd.), and a Memsic MXA2100A accelerometer (cost $\approx$ \$8, Memsic, Inc.), as shown in Fig. 1. At first glance, our approach is similar to that used by Baerveldt and Klang [1] and by Rehbinder and Hu [2]. However, we found that none of the existing methods produced the accuracy or bandwidth that we required. Baerveldt and Klang assume the inclinometer is a first-order low-pass filter with time constant $\tau = 0.53$ s. This model is shown to be good for lower frequency motions (in their case 0.15–1.5 Hz), but the first-order assumption is not valid at higher frequencies. Rehbinder and Hu use a nonlinear observer to not only estimate attitude, but also model their inclinometer as a first order low-pass filter. Again, their observer is shown to perform well at frequencies around 1 or 2 Hz. Because our robot systems potentially operate at frequencies approaching 5 Hz, we needed to develop a significantly improved state estimation technique.

Our method has four main differences from previous approaches: 1) a higher fidelity model for the inclinometer was developed using both a physics-based model and a frequency-domain system identification technique; 2) an optimal state estimator (Kalman filter) is used that continuously combines the measurements to obtain more accurate angle and angular rate information; 3) the inherent bias of the gyroscope is identified, and compensated for, online; and 4) translational acceleration is explicitly accounted for in the tilt-sensing state estimator.

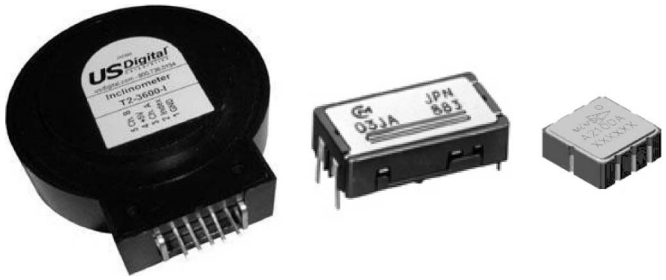

Fig. 1. U.S. Digital inclinometer (left), Murata gyroscope (middle), and Memsic accelerometer. For relative size of inclinometer and gyroscope, note that connection wires are 0.1 in apart.

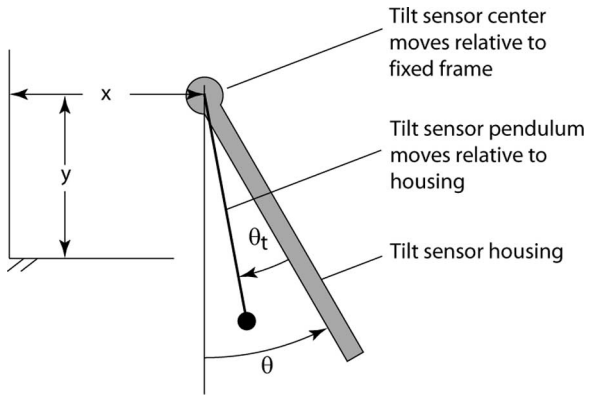

Fig. 2. Modeling the inclinometer as a simple pendulum.

II. Modeling and Performance Characteristics of the Sensors

A. Inclinometer

The US Digital optical inclinometer measures the angular position of a pendulum relative to its housing. An encoder with a resolution of 7200 counts/revolution (after quadrature) is used to track the position of the pendulum. Fig. 2 shows a schematic representation of the inclinometer. Because the pendulum has its own dynamics, the desired inclination angle, $\theta_{\rm t}$, output from this sensor is accurate only at low frequencies. To investigate the dynamics of our inclinometer, we mounted a hinge joint to a fixed table (see Fig. 3) and measured the true angle of the pendulum with an optical encoder. We then oscillated the joint with an increasing frequency "chirp signal." The chirp input starts at 0.25 Hz and ends at approximately 4.6 Hz over a period of 107 s. Sensor outputs were sampled at 500 Hz. The inclinometer shown in Fig. 3 was mounted at the axis of rotation so that it did not undergo any base acceleration during the system identification process. Fig. 4 shows the output of the inclinometer as a function of time as the actual inclination angle (measured with an encoder and used for comparison only) varies with the increasing frequency chirp. At high frequencies, the inclinometer exhibits distortion in both magnitude and phase.

To obtain the dynamic model for the system, consider the tilt sensor to be a simple pendulum with damping and assume that there is a translational acceleration of the base defined by $(\ddot{x}, \ddot{y})$ as shown in Fig. 2. Let θ be the actual angle of the sensor and $\theta_{\rm t}$ be the pendulum angle, which is the tilt sensor output, as seen in Fig. 2. The differential equation for the system is

$$J(\ddot{\theta} - \ddot{\theta}_{\rm t}) = c\dot{\theta}_{\rm t} - mgl\sin(\theta - \theta_{\rm t}) - ml(\ddot{y}\sin(\theta - \theta_{\rm t}) + \ddot{x}\cos(\theta - \theta_{\rm t}))$$

for some damping coefficient c, length from pivot to mass center l, mass m, and inertia about the pendulum pivot J. Assuming small $\theta - \theta_{\rm t}$, $\sin(\theta - \theta_{\rm t}) \approx \theta - \theta_{\rm t}$ and $\cos(\theta - \theta_{\rm t}) \approx 1$. We further assume that the nonlinear term $\ddot{y}(\theta - \theta_{\rm t})$ that results from these assumptions is negligible. The differential equation simplifies to

$$J(\ddot{\theta} - \ddot{\theta}_{\rm t}) = c\dot{\theta}_{\rm t} - mgl(\theta - \theta_{\rm t}) - ml\ddot{x}.$$

If we define $\alpha_1 \equiv c/J, \alpha_2 \equiv mgl/J,$ and $\gamma_1 \equiv \alpha_2/g$ and take $\beta_0 = 1, \beta_1 = 0,$ and $\beta_2 = \alpha_2$, the transfer function representation of the linearized equations of motion for this system has the form

$$\Theta_{\rm t}(s) = \frac{\beta_0 s^2 + \beta_1 s + \beta_2}{s^2 + \alpha_1 s + \alpha_2}\Theta(s) + \frac{\gamma_1}{s^2 + \alpha_1 s + \alpha_2}X_{\rm a}(s) \quad (1)$$

where $\Theta_{\rm t}(s)$, $\Theta(s)$, and $X_{\rm a}(s)$ are the Laplace transforms of the $\theta_{\rm t}(t)$, $\theta(t)$, and $\ddot{x}(t)$ signals, respectively.

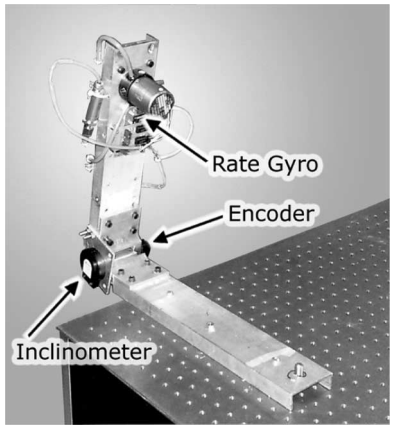

Fig. 3. Test apparatus for encoder, inclinometer, gyroscope. A chirp test signal was applied to the hardware by a pneumatically actuated controller.

B. Gyroscope and Accelerometer

To investigate the dynamic characteristics of the Murata gyroscope, we mounted it to the same test apparatus as used for the inclinometer experiments and applied the same chirp test signal. The output of a Murata gyro (approximately scaled to units of rad/s) is shown in the top plots of Fig. 5. Also shown in the figure is the signal obtained from a backward finite difference of the joint encoder signal. This signal was also passed through a first-order low-pass filter with a cutoff frequency of 20 Hz. From the plots, it appears that a bias of about 3 rad/s is present in the gyro output signal. We then subtracted this value from the gyro signal, and integrated this difference to obtain the

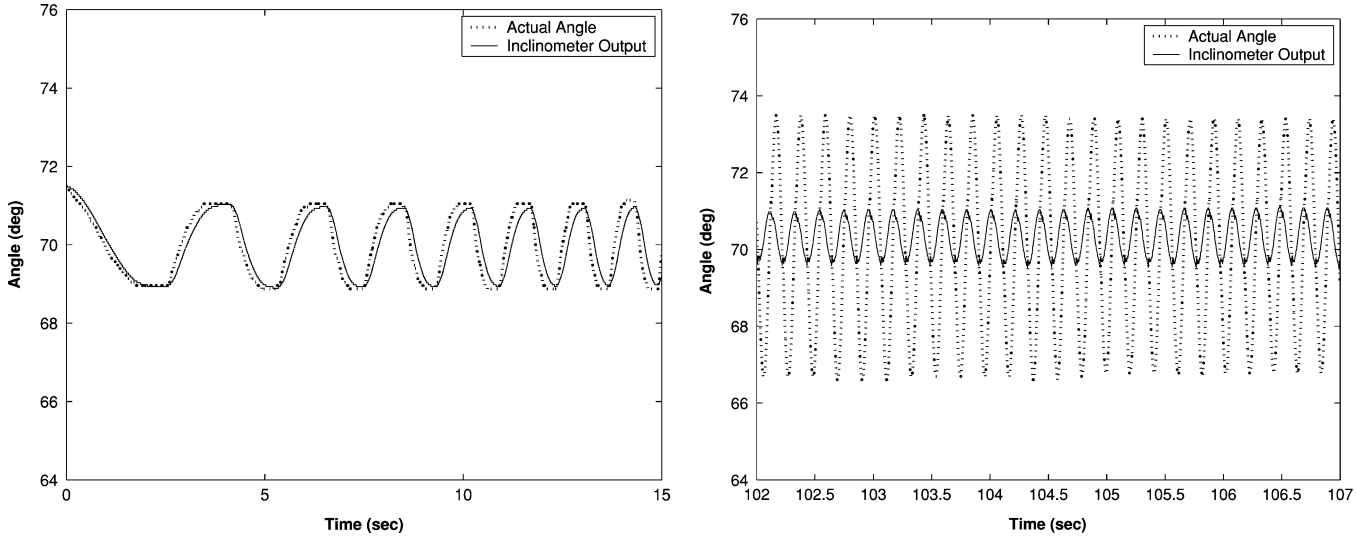

Fig. 4. Tilt angle measured with encoder and inclinometer in a chirp motion. The left-hand plot shows the first 15 s of motion and the right-hand plot shows the last 5 s.

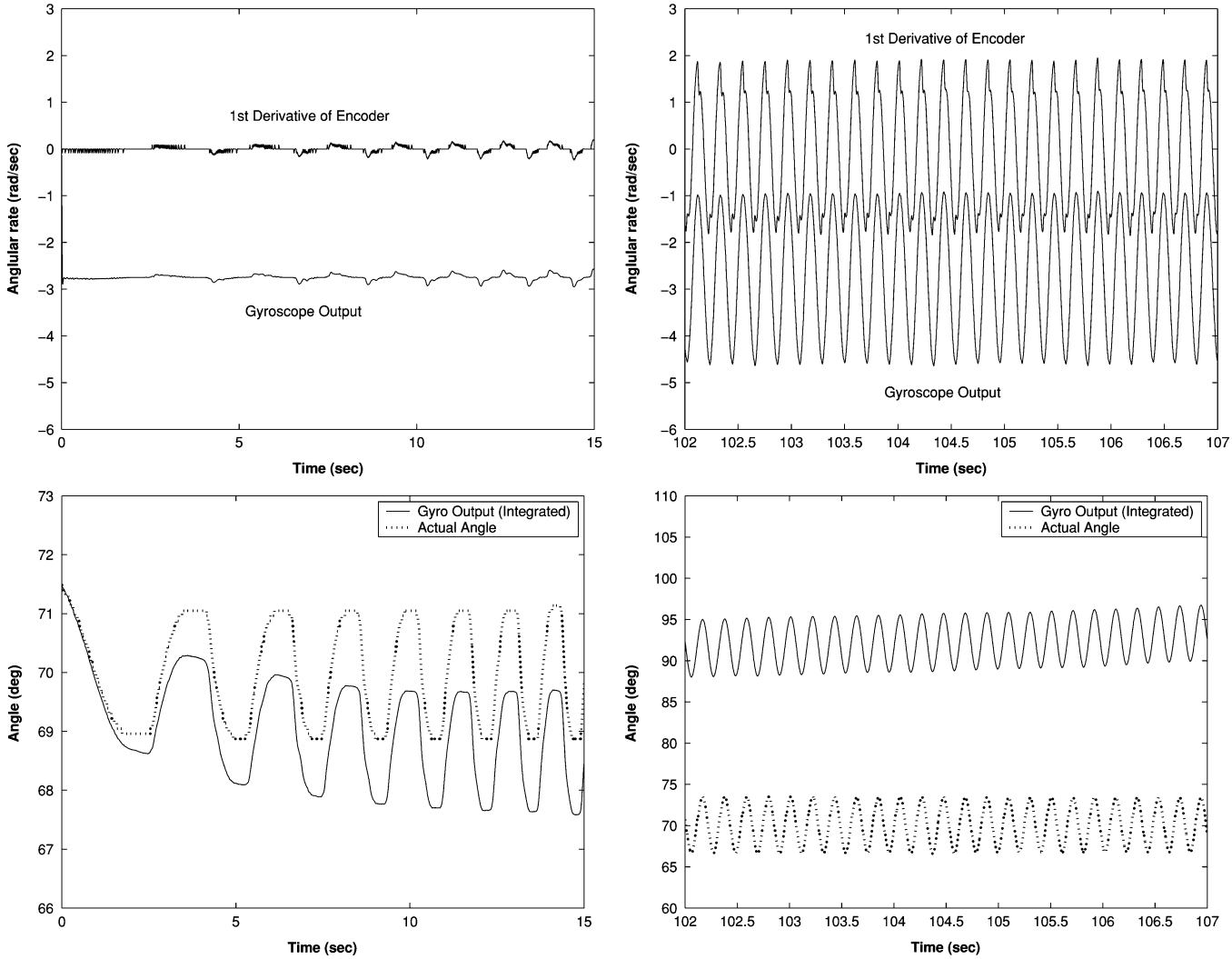

Fig. 5. Raw output from the gyroscope and the differentiated and filtered output of the encoder for the low- and high-frequency parts of the chirp input (top). Integral of the gyro signal minus a constant drift and the joint encoder signals (bottom).

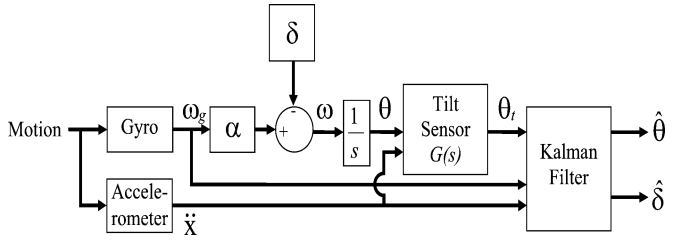

Fig. 6. Block diagram of estimation system with no noise input. The measured signals are the outputs of the gyroscope $\omega_{\rm g}$, the accelerometer $\ddot{x}$, and the tilt sensor $\theta_{\rm t}$.

bottom plots shown in Fig. 5. The plots show a significant error in magnitude from the true angle (as measured by the encoder). It is clear that the gyro sensor introduces a drift to the signal due to the unknown bias term, and this bias might be slowly varying with time.

To obtain the translational acceleration $\ddot{x}$ in (1), we used a two-axis accelerometer made by Memsic. The bandwidth for this device is 30 Hz.

III. Observer Design for Accurate Tilt Measurement

In this section, we construct an optimal observer (Kalman filter) that considerably improves tracking of the tilt angle θ by combining the inaccurate measurements of the gyro and tilt sensors. The observer reconstructs the states of the angle-measuring system as depicted in Fig. 6. In this system, the tilt sensor is described by the second-order transfer function (1). The observable-canonical-form state-space realization for (1) can be written as follows:

$$\begin{bmatrix}\dot{x}_1\\ \dot{x}_2\end{bmatrix} = \begin{bmatrix}-\alpha_1 & 1\\ -\alpha_2 & 0\end{bmatrix}\begin{bmatrix}x_1\\ x_2\end{bmatrix} + \begin{bmatrix}\beta_1-\beta_0\alpha_1\\ \beta_2-\beta_0\alpha_2\end{bmatrix}\theta + \begin{bmatrix}0\\ \gamma_1\end{bmatrix}\ddot{x}$$

$$\theta_{\rm t} = [1 \quad 0]]\begin{bmatrix}x_1\\ x_2\end{bmatrix} + \beta_0\theta + v_{\rm t}. \tag{2}$$

In (2), $v_{\rm t}$ represents the inclinometer measurement noise. Next, the gyro sensor is described by the equation

$$\omega_{\rm g} = \frac{1}{\alpha}(\omega+\delta) + v_{\rm g} \tag{3}$$

where ω and $\omega_{\rm g}$ are actual and measured angular velocities, δ and α are the bias and scaling factors in the gyro sensor, respectively, and $v_{\rm g}$ represents the gyro measurement noise. Finally, to model the gyro bias, we use the equation

$$\dot{\delta} = v_{\rm b}. \tag{4}$$

In (4), v_b is white noise that is introduced in the model mainly for the optimal observer problem to be well posed and solvable; however, it also allows the gyro bias to fluctuate to some extent, which is consistent with our experience in practice.

The above equations together with the relation

$$\dot{\theta} = \omega$$

give the following state-space equations for the angle measuring system:

$$\begin{bmatrix}\dot{\delta}\\ \dot{\theta}\\ \dot{x}_1\\ \dot{x}_2\end{bmatrix} = \begin{bmatrix}0 & 0 & 0 & 0\\ -1 & 0 & 0 & 0\\ 0 & \beta_1-\beta_0\alpha_1 & -\alpha_1 & 1\\ 0 & \beta_2-\beta_0\alpha_2 & -\alpha_2 & 0\end{bmatrix}\begin{bmatrix}\delta\\ \theta\\ x_1\\ x_2\end{bmatrix} + \begin{bmatrix}0 & 0\\ \alpha & 0\\ 0 & 0\\ 0 & \gamma_1\end{bmatrix}\begin{bmatrix}\omega_{\rm g}\\ \ddot{x}\end{bmatrix} + \begin{bmatrix}0 & 1 & 0\\ 0 & 0 & -\alpha\\ 0 & 0 & 0\\ \gamma_1 & 0 & 0\end{bmatrix}\begin{bmatrix}v_{\rm x}\\ v_{\rm b}\\ v_{\rm g}\end{bmatrix}$$

$$\theta_{\rm t} = [0 \quad \beta_0 \quad 1 \quad 0]]\begin{bmatrix}\delta\\ \theta\\ x_1\\ x_2\end{bmatrix} + v_{\rm t}$$

where we also added measurement noise $v_{\rm x}$ to the accelerometer signal $\ddot{x}$.

This system is of the standard form

$$\dot{z} = Az + Bu + B_{\rm v}v$$

$$\theta_{\rm t} = Cz + v_{\rm t}$$

with $z \equiv [\delta \ \ \theta \ \ x_1 \ \ x_2]^T, u \equiv [\omega_g \ \ \ddot{x}]^T, v \equiv [v_{\rm x} \ \ v_{\rm b} \ \ v_{\rm g}]^T$, and $A, B, B_{\rm v}$, and C defined in the obvious way. Note that in this formulation, the unknown bias δ and the tilt angle θ are states of the system. The inputs are the measured gyro signal $\omega_{\rm g}$, the measured acceleration signal $\ddot{x}$, and the measurement noises $v_{\rm x}, v_{\rm b}, v_{\rm g}$, and $v_{\rm t}$. Finally, the output of the system is the measured inclinometer signal $\theta_{\rm t}$. Next, we consider a standard state estimator (observer) of the form

$$\dot{\hat{z}} = A\,\hat{z} + K(\theta_{\rm t} - C\,\hat{z}) + Bu. \tag{5}$$

Selecting the gain vector K such that $A-KC$ is an asymptotically stable matrix guarantees that the state reconstruction error $z-\hat{z}$ remains bounded, and in the absence of the noise signals, that $z-\hat{z}$ converges asymptotically to 0. We actually considered an optimal observer (Kalman filter) that minimizes the mean square tracking error $E[(z-\hat{z})^T(z-\hat{z})]$ and can be readily designed by considering the dual-state regulator problem (for example, see [8]) and using MATLAB's lqr command. In the cost function of the latter problem, the state weighting matrix $Q = \text{diag}\{W_{\rm b}^2,\ \alpha^2 W_{\rm g}^2,\ \gamma_1^2 W_{\rm x}^2,\ \gamma_1^2 W_{\rm x}^2\}$ and the control weighting matrix $R = W_{\rm t}^2$, where $W_{\rm b}, W_{\rm g}, W_{\rm x}$, and $W_{\rm t}$ are the root mean square (RMS) values of the bias $v_{\rm b}$, gyro $v_{\rm g}$, accelerometer v_x, and tilt sensor $v_{\rm t}$ noises, respectively, all assumed to be modeled as white noise. The values of $W_{\rm b}^2, W_{\rm g}^2, W_{\rm x}^2$, and $W_{\rm t}^2$ are actually used to tune the performance of the observer, namely, to tradeoff the speed of state reconstruction with the extent of observer bandwidth and its susceptibility to measurement noise. We found that the values $W_{\rm b}^2 = 1.0, W_{\rm g}^2 = 0.866, W_{\rm x}^2 = 1.376$, and $W_{\rm t}^2 = 0.5$ provide

such a reasonable tradeoff, resulting in the observer gains $K = [-1.4142 \quad 2.2286 \quad 44.8444 \quad 212.6269]^T$.

IV. System Identification of Inclinometer Dynamics

From (5), it is clear that the observer acts as a filter that combines the imperfect gyro $\omega_{\rm g}$, inclinometer $\theta_{\rm t}$, and accelerometer $\ddot{x}$ signals to produce an improved estimate of the tilt angle θ in terms of the estimated state $\hat{z}(2)$. Note that the observer automatically estimates the gyro bias δ in terms of $\hat{z}(1)$ and compensates for it. However, to use this scheme, we need to have the observer parameters α_1, α_2, and $\beta_0, \beta_1, \beta_2$ (recall that $\gamma_1 = \alpha_2/g$), that is, the inclinometer transfer function in (1) from θ to $\theta_{\rm t}$. We employ a frequency domain identification technique to obtain this transfer function. More specifically, the output of the integrator/inclinometer system in Fig. 6 is $\theta_{\rm t}$, while the inputs to this system (neglecting measurement noise) are $\ddot{x}$ and ω, with the latter being related from (3) to the gyro measurement $\omega_{\rm g}$ by

$$\omega = \alpha\omega_{\rm g} - \delta.$$

For the moment, we assume that $\delta = 0$ and $\alpha = 1$, i.e., $\omega = \omega_{\rm g}$, and we will shortly see that the value of the bias δ does not affect the frequency domain identification process, while the actual scaling α can be easily determined through this process. We used data for the identification procedure from the experiment in Section V-A, where the translational acceleration $\ddot{x}$ is zero. Thus, only the gyro $\omega_{\rm g}$ and inclinometer measurements $\theta_{\rm t}$ are used in the identification; however once identified, the inclinometer dynamics are used in the observer (5) in all situations, where $\ddot{x}$ might not be zero (experiments in Sections V-B and V-C.) The measured signals $\omega_{\rm g}$ and $\theta_{\rm t}$ are produced by applying a chirp input as discussed in Section II-A. Over the time horizon $T = 107$ s with a sampling frequency $f = 500$ Hz, we collected $N = 53\,501$ samples. We then computed the discrete fourier transforms (DFT) of $\omega_{\rm g}(kT_p)$ and $\theta_{\rm t}(kT_{\rm p}), k = 0, \ldots, 53\,500$, where $T_{\rm p} = 1/f = 0.002$ s using MATLAB's *fft* command. Finally, we obtained samples of the frequency response $G(jk\Omega_{\rm p}), k = 0, \ldots, 53\,500$ of integrator/inclinometer combination in Fig. 6 as the ratio of the DFT of $\theta_{\rm t}$ (output) to the DFT of $\omega_{\rm g}$ (input—since we assume for now $\omega = \omega_{\rm g}$), where $\Omega_{\rm p} = (2\pi/T) = 0.0093$ rad/s.

We should remark that a number of factors contribute to errors in the estimation of the samples $G(jk\Omega)$. First, since the chirp input has its power over frequencies from 0.25 to 4.6 Hz, we can expect to be able to reliably identify the frequency range from about 0.2 to 5 Hz. Then, errors may be introduced because of aliasing and leakage [9]. Aliasing results if the sampling frequency is less than twice the highest frequency in the signal being sampled. However, we do not expect aliasing to be an issue since we used an anti-aliasing filter with a cutoff frequency of 50 Hz. This means that our sampling rate of 500 Hz is ten times higher than the expected bandwidth of the measured signals. Leakage refers to the ripple-like effect in the frequency response obtained from using (out of practical necessity) the Fourier transformation on time-domain data over a finite horizon instead of an infinite one. It can be reduced by increasing N, or by using windowing filters at the expense of "smearing" the frequency response [9]. Indeed, since we did not employ any data windowing, some rippling in the frequency samples can be observed but the curve fitting approach employed to obtain the transfer function from the samples $G(jk\Omega_p)$ tends to smooth out this effect.

Next, the experimental frequency response curve [samples $G(jk\Omega)$] is fitted with a rational transfer function by minimizing a least squares criterion

$$\min_{\alpha_k, \beta_l} \sum_{i=N_1}^{N_2} w_i \left| G(j\Omega_i) - \frac{\beta_0(j\Omega_i)^m + \beta_1(j\Omega_i)^{m-1} + \cdots + \beta_m}{(j\Omega_i)^n + \alpha_1(j\Omega_i)^{n-1} \cdots + \alpha_n} \right|^2 \tag{6}$$

with $k = 1, \ldots, n$ and $l = 0, \ldots, m$ and where n, m are the number of poles and zeros, respectively, of the model selected by the user. Also in (6), the w_i are weights that are selected to emphasize certain frequencies such as those where the experimental data show resonances/notches (see Fig. 7). We employed a recursive algorithm reported in [10], but using a parametrization of the numerator and denominator polynomials of the fit in terms of Chebychev polynomials [11], [12]; the Chebychev parametrization alleviates the numerical difficulties that the standard parametrization in (6) can suffer from because of an extended frequency range and/or high polynomial orders n, m. As discussed above, we took N_1 and N_2 in (6) to fit the available data from 0.2 to 5 Hz. Furthermore, we scaled the experimental frequency response samples $G(j\Omega_i)$ by $j\Omega_i$ before curve fitting was attempted so that the resulting transfer function describes exactly the inclinometer dynamics in (1). This scaling in effect corresponds to scaling $G(s)$, the integrator/inclinometer transfer function, by s, thus canceling the integrator in the measured frequency response between ω and $\theta_{\rm t}$ in Fig. 6.

We now remark on why the gyro bias δ does not affect this procedure, and how the scaling α can be accurately determined. First, note that the bias introduces a delta function at $s = 0$ in the frequency response and that curve fitting is attempted from 0.2 to 5 Hz so that the bias has no effect on the identification. Then, note that α has the effect of scaling the experimental frequency response and the curve fit. Since it is known that the dc gain of the inclinometer is 1, we simply identify α as the scaling required to make the resulting curve fit have a dc gain of 1.

Fig. 7 shows the best-fit transfer functions of varying degrees, starting with one pole and no zeros (top left), two poles and no zeros (top right), and two poles and two zeros (bottom). Note that the first-order model, seen in Fig. 7, is a good fit from about 0.3 to about 2 Hz, but misses the notch apparent in the data at approximately 3.7 Hz. The bottom plot in the figure shows an excellent fit within the 0.2–5 Hz range, with identified transfer function

$$G_{\rm p}(s) = \frac{1.024s^2 - 0.1791s + 528.4}{s^2 + 65.86s + 528.4}.$$

Our identified observer parameters are $\alpha_1 = 65.86, \alpha_2 = 528.4, \beta_0 = 1.024$ and $\beta_1 = -0.1791$. As described previously, β_2 was forced to equal to α_2 so that the dc gain of the inclinometer is one. We observe that $G_{\rm p}(s)$ is consistent with (1), and

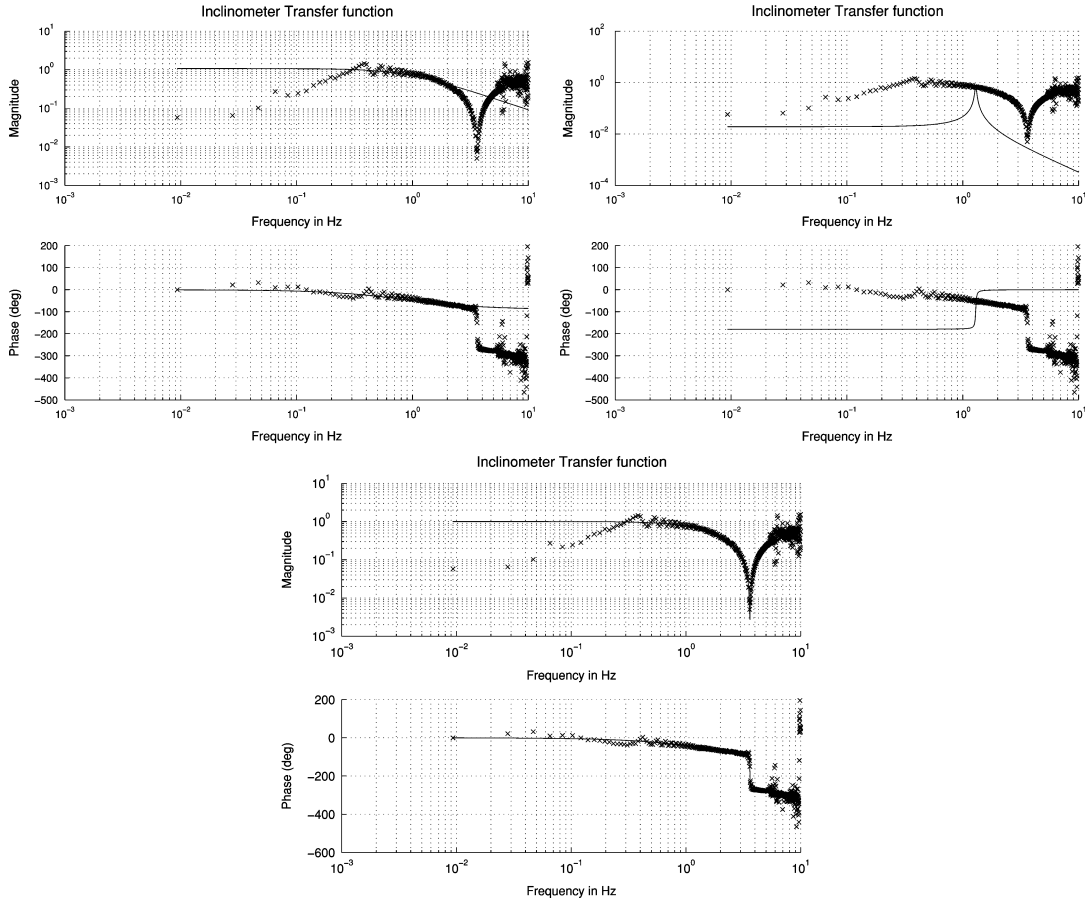

Fig. 7. Best-fit transfer functions of varying degrees, starting with one pole and no zeros (top-left), two poles and no zeros (top-right), and two poles and two zeros (bottom).

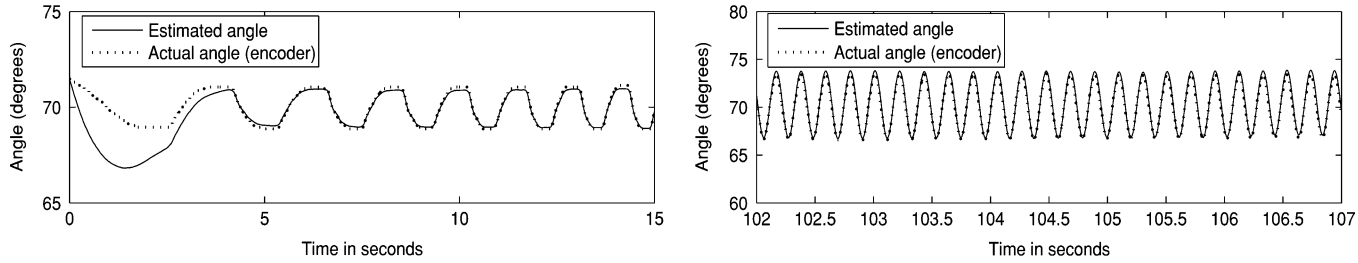

Fig. 8. Observer designed from tilt sensor transfer function, two poles and two zeros (left, first 15 s; right, last 5 s).

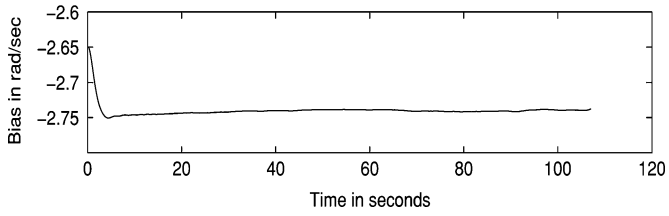

Fig. 9. Observer's estimate of the gyro bias during the chirp motion.

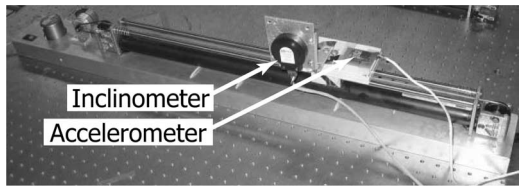

Fig. 10. Experimental setup for horizontal translation.

less small differences in the high-frequency gain and the small damping in the numerator (i.e., $\beta_0 = 1.024$ and $\beta_1 = -0.1791$ instead of the ideal modeling values $\beta_0 = 1$ and $\beta_1 = 0$) are found. We also remark that the natural frequency of the zeros of the model is $(\sqrt{528.4}/2\pi) = 3.66$ Hz, well within the range of device, which shows the importance of using the more accurate model. Finally, the gyro scaling is also identified to have a value of $\alpha = 0.76$ based on the approach discussed above.

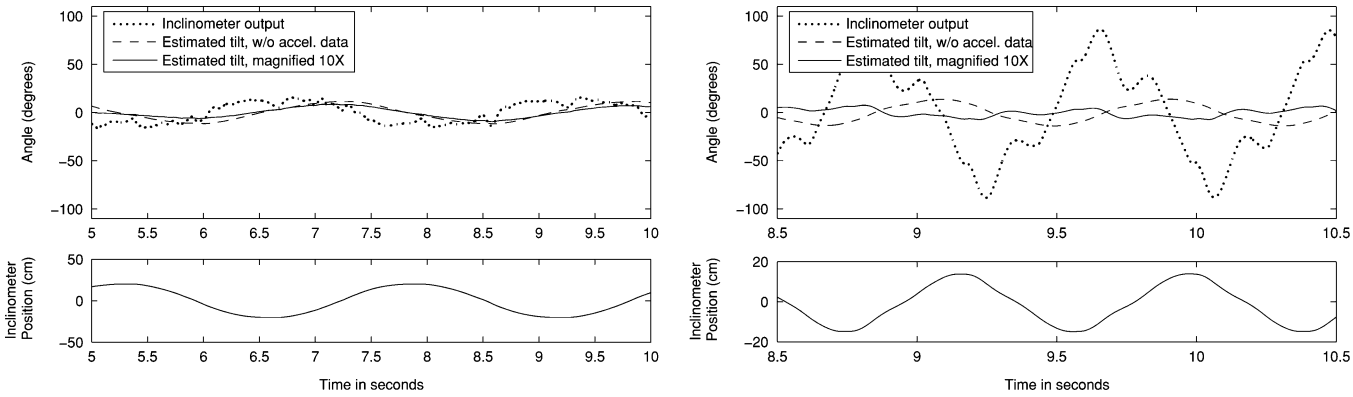

Fig. 11. Angle estimate as sensor accelerates with $\ddot{x} = \pm 0.98$ m/s^2 (left) and with $\ddot{x} = \pm 9.8$ m/s^2 (right).

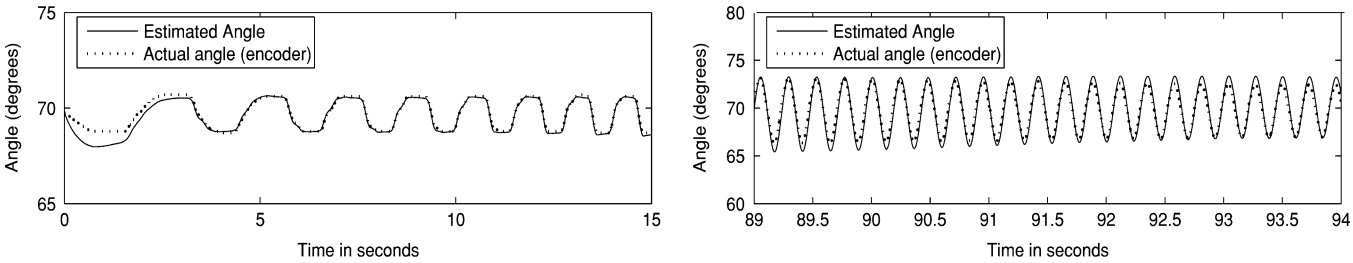

Fig. 12. Observer designed from tilt sensor transfer function, with inclinometer placed off the axis of rotation (left, first 15 s; right, last 5 s).

V. Experimental Results

A. Planar Rotation

We first tested the observer design from Section III in the case of pure rotation of the tilt sensor with zero base acceleration. The tilt sensor was mounted along the axis of rotation as shown in Fig. 3. The data from the same chirp signal used for the system identification in Section IV was input into the observer, and the tilt angle estimate was compared to the measured tilt angle. Fig. 8 shows the estimated tilt and the actual angle at low and high frequencies. For the initial conditions, we set the estimated angle to be close to the actual angle, but introduced a significant error in the initial estimate for the gyro bias signal. This error caused the observed angle to deviate from the true angle during the first few seconds of the estimator's transient response. The last 5 s of the chirp motion shows our observer tracking a signal of frequencies exceeding 4 Hz. Fig. 9 shows the estimate of the gyro bias signal to converge to a value of $\delta = -2.74^\circ$/s in about 4 s. It also shows that the observed bias signal varies somewhat during normal operation.

B. Horizontal Translation

The results seen in Fig. 8 are valid for the case when the inclinometer rotates without translating. The following experiments introduce translational acceleration to the inclinometer. For the first experiment, we fixed the inclinometer and an accelerometer to a sliding platform oriented to move in the horizontal direction as shown in Fig. 10. Using a pneumatic actuator, we accelerated and decelerated the platform in a square wave with $(\ddot{x} = \pm a,)$ creating a smooth back and forth motion (see the translational motion shown in the lower plots of Fig. 11). Ideally, the observer should output a tilt angle estimate of zero degrees since the inclinometer is not rotating. In Fig. 11, we plot the inclinometer output, the tilt angle estimate assuming that the acceleration is zero, and the tilt angle estimate using the the measured acceleration signal. In both the figures, we magnified the tilt angle estimate by a factor of 10 since it was very close to zero. The figure shows a less than 1° deviation from zero for the case when $a = 0.1g$ (left plot) and less than a 2° error for $a = 1g$ (right plot). In both cases of low and high accelerations, the angle estimate was roughly ten times as accurate compared to the angle estimate based on the assumption that the acceleration was zero. Also note that the inclinometer is making large oscillations for the case of $1g$ accelerations, and the estimator still works well.

C. Translation and Rotation

In the last experiment, we used the original test setup shown in Fig. 3, with the tilt sensor placed 10 cm from the axis of rotation. As before, the device was oscillated in a chirp motion around the 70° (from horizontal) position. This motion created accelerations of the order of $1g$ in both the x- and y-directions. The accelerations were due to the angular velocity and angular acceleration of the rotating arm. Rather than using the accelerometer, we computed the linear acceleration of the tilt sensor from the measured encoder signal and its derivatives. Data from all three sensors were fed to the observer, giving the results seen in Fig. 12. The plots show that at both low (<1 Hz) and high (>3 Hz) frequencies, the estimated signal deviates from the actual signal by no more than 1°. This result shows that satisfactory performance of the observer is obtained

even in the case when considerable translational accelerations are present in both the x- and y-directions.

VI. Conclusion

We have outlined a method for combining data from an inclinometer, a rate gyro, and an accelerometer to produce an accurate angle measurement, even when translational accelerations are substantial. This method involves modeling the sensors as linear time-invariant systems. The rate gyro is modeled as the derivative of the angle to be estimated, plus an unknown bias and scaling. The tilt sensor is modeled as a second-order proper transfer function from the input angle to the tilt sensor output angle. The parameters of this transfer function are obtained by fitting its frequency response to the experimental frequency response of the tilt sensor to a chirp motion. Then, an optimal linear state estimator is constructed that estimates the gyro bias, and infers the correct angle from the output of all three sensors. Our method is unique in that it cancels the gyro bias more effectively than a simple high-pass filter. Furthermore, our more realistic model of the inclinometer allows for state observation at higher frequencies than has been reported in previous research.

References

[1] A. J. Baerveldt and R. Klang, "A low-cost and low-weight attitude estimation system for an autonomous helicopter," in *Proc. IEEE Conf. Intelligent Engineering Systems*, 1996, pp. 391–395.

[2] H. Rehbinder and X. Hu, "Nonlinear state estimation for rigid-body motion with low-pass sensors," *Systems & Control Letters*, Elsevier, Netherlands, vol. 40, no. 3, pp. 183–190, Jul. 5, 2000.

[3] H. Rehbinder and X. Hu, "Drift free attitude estimation for accelerated rigid bodies," *Automatica*, vol. 40, pp. 653–659, 2004.

[4] L. Ojeda and J. Borenstein, "FLEXnav: Fuzzy logic expert rule-based position estimation for mobile robots on rugged terrain," in *Proc. 2002 IEEE Int. Conf. Robotics and Automation*, Washington, DC, May2002, pp. 317–322.

[5] J. Leavitt *et al.*, "Robust balance control of an under-actuated, one-legged hopping robot," Univ. CaliforniaWiley, Irvine, M.S. Project Rep., 2003.

[6] H. J. Luinge *et al.*, "Estimation of orientation with gyroscopes and accelerometers," in *Proc. First Joint 21st Annu. Conf. and Annu. Fall Meeting Biomed. Eng. Soc. BMES/EMBS Conf., Eng. Med. Biol.* 13–16, 1999, vol. 2, p. 844.

[7] J. Vaganay *et al.*, "Mobile robot attitude estimation by fusion of inertial data," in *Proc. IEEE Int. Conf. Robot. Automat.* 2–6, 1993, vol. 1, pp. 277–282.

[8] H. Kwakernaak and R. Sivan, *Linear Optimal Control Systems*. New York: Wiley, 1972.

[9] E. Brigham, *The Fast Fourier Transform and Its Applications*. Englewood Cliffs, NJ: Prentice-Hall, 1988.

[10] C. K. Sanathanan and J. Koerner IEEE Trans. Autom. Control, vol. 8, no. 1, pp. 56–58.

[11] J. L. Adcock, "Analyzer synthesizes frequency response of linear systems," *Hewlett-Packard J.*, pp. 25–32, Jan. 1987.

[12] J. L. Adcock, "Curve fitter for pole-zero analysis," *Hewlett-Packard J.*, pp. 33–36, Jan. 1987.

John Leavitt (A'82–M'88) received the M.S. degree in mechanical and aerospace engineering from the University of California, Irvine, in 2003. He is currently pursuing the Ph.D. degree at the same university.

His research interests include state estimators, fluid powered robots, and semiactive dampers for use with building structures.

Athanasios Sideris (S'80–M'85) received the diploma degree in electrical and mechanical engineering from the National Technical University, Athens, Greece, in 1980, the M.S. and Ph.D. degrees in electrical engineering, in 1981 and 1985, respectively, and the M.S. degree in mathematics, in 1986, all from the University of Southern California, Los Angeles.

From 1986 to August 1992, he was an Assistant Professor at the Department of Electrical Engineering, California Institute of Technology. In January 1992, he joined the Department of Mechanical and Aerospace Engineering, University of California, Irvine, where he is currently a Professor. His current research interests include robust control theory, optimization and optimal control, learning algorithms, and neural networks.

James E. Bobrow (M'84) received the M.S. and Ph.D. degrees from the University of California Los Angeles, in 1979 and 1983, both in engineering.

From 1983 to 1984, he was a Senior Programmer Analyst at McDonnell Douglas Automation Company, where he developed CAM software for the Unigraphics system. In July 1984, he joined the University of California, Irvine, (UCI) as an Assistant Professor and conducted research in robotics and applied control systems. During 1991–1992, he was a Visiting Associate Professor in the Computer Science Department, Stanford University, where he investigated applications of numerical optimization algorithms to learning systems. He has created robots and automation devices for several start-up companies, including Robomedica, Inc., and Cobra Technologies. He is currently a Professor of mechanical and aerospace engineering at the UCI.

Dr. Bobrow serves on the Engineering Advisory Board of Robomedica, Inc., and has served on the program committees or organizing committees of the leading conferences in control systems and robotics.